Egyptian Geophysical Society
EGS Journal, Vol. 12, No. 1, 113-121 (2014)

DESIGN AND APPLICATION OF AN AUTOMATIC TECHNIQUE FOR MANEUVERS CORRECTIONS OF AIRBORNE MAGNETIC DATA

A.S.S. EL-KABBANI(1), K.G. ABDEL-KADER(2), A. A.M. ISMAIL(3), F.A.S. SOLIMAN(3), and A.M. ABDEL-MAKSOUD(3)

(1) Electronics and Communications Dept., Fac. of Eng., Al-Azhar University, Nasr-City, Cairo
(2) South Cairo Electricity Distribution Company, Ministry of Electricity and Energy,
(3) Exploration Sector, Nuclear Materials Authority, Qattamya-Maadi Road, Cairo, Egypt.

تصميم وتطبيق طريقة آلية لعمل تصحيحات المناورات لمعطيات المسح المغناطيسى الجوى

الخلاصة: تعتبر الشوشرة المغناطيسية الناتجة من حركة الطائرة أثناء المسح المغناطيسي الجوي من أهم العوامل التي تتحكم في جودة البيانات حتى ولو كانت الطائرة المستخدمة صغيرة الحجم، لذا فان معالجة هذه الشوشرة تعتبر من العوامل الأساسية لتحسين دقة البيانات وكان هذا هو هدف وخطة البحث للوصول الي طريقة تعالج هذه الشوشرة. لقد تم تصميم طريقة جديدة لمعالجة هذه الشوشرة ومقارنتها بالطرق التقليدية. وقد أظهرت هذه الطريقة سهولة في المعالجة ودقة في النتائج حيث بينت النتائج معامل خطأ قدره ٠,٣٥١١ نانو تسلا وهي نتيجة جيدة جدا مقارنة بحدود معامل الخطأ المستخدم بالطرق التقليدية وهو واحد نانو تسلا.

ABSTRACT: *In aero-magnetic survey, magnetic noise from the flying platform is one of the factors that determine the data's accuracy. Normally, light aircraft, which are often used as the platforms in aero-magnetic survey, can cause remarkable magnetic interference. Removing this kind of interference is important to improve the data's accuracy. So, in the present paper, an approach in aero-magnetic compensation was investigated. The compensation results have been evaluated, verified, and compared with the traditional compensation methods. The results of the proposed approach were shown to be easy to process with high efficiency. Standard flying and coefficients extractions can easily be calculated, based on physical and mathematical methods, and the accuracy relies only on the efficiency of the numerical calculations. The advantage of this approach is that the accuracy can be significantly improved since the geomagnetic field is far outweighs the magnetic interference. Finally, an error factor value of 0.3513 was obtained, compared with that value of 1.0, which, is presently obtained applying traditional techniques.*

Outline Airborne Geophysical Survey:

It is expected that data resulting from the geophysical surveys will help manage our environment and support sustainable natural resource development by providing more information about our soils, sediments, waters and rocks, as well as for landmines exploration [1-4]. In this concern, the geophysical aircraft carried a range of geophysical equipment that maps the geological characteristics of rocks and soils. Such information will improve the understanding of our natural environment. It will contribute to and therefore benefit sustainable land use planning decisions. The survey will also help identify potential natural hazards and map certain forms of contamination.

The main systems on board the geophysical aircraft are magnetic, radiometric (gamma ray spectrometry), electromagnetic, and gravity, which measure different physical properties of the earth (Fig. 1). In the case of the magnetic system, which is the point of interest within the present paper, the instrument measures the strength of the magnetic field of the earth, which provides information on the different rock types under the ground (in general the more iron in the rock the greater the magnetic field strength). It also allows geologists and the geophysicists to identify different structures in the earth. Such faults or fractures are often pathways where water, mineralized fluids (to form mineral deposits) or radon travel through the earth.

2.0 .Airborne Magnetic Survey of Egypt

The airborne geophysical survey of Nuclear Materials Authority of Egypt mainly comprises a Beechcraft KingAir B200 equipped with the state-of the-art airborne geophysical system, as well, a complete navigational and data flight recovery system.

2.1. Aircraft:

The Beechcraft KingAir B200 features a 305-knot maximum cruise speed. The engine holds 850-shp flat rating insuring a much higher altitude, improving climb rate (2450 ft/min), range with maximum fuel and reserves 3658 km, and cruise performance under almost all flight scenarios.

2.2. Geophysical Equipments:

The survey equipments are multichannel gamma ray spectrometer, cesium vapor multi-sensor magnetometer, and gravimeter. For interest, Throughout the present scientific work, further light will be shed upon the airborne magnetic survey and its problems. In this concern, a brief description about the system of interest will be presented.

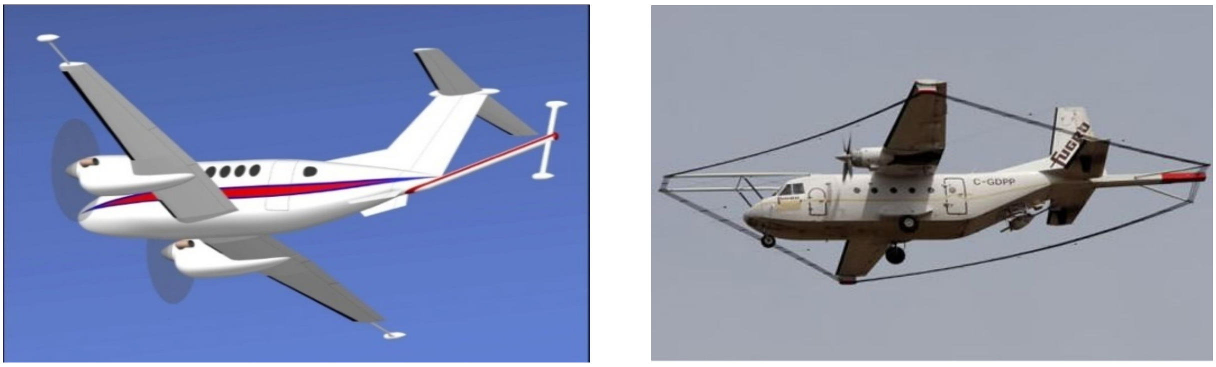

(a) (b)

Fig. (1): Airborne magnetic (a) and electromagnetic (b) survey aircraft.

2.2.1. MS-4 Magnetometer:

The MMS-4 is an intelligent high sensitivity, high resolution magnetometer processor. It is upgradeable to manage and process as many as four cesium magnetometers (such as the CS-3). It contains a continuous frequency processing input module with a signal decouples and power control circuitry. The MMS-4 was originally designed as a key component of Pico Envirotec's Airborne Geophysical Information System (AGIS). The processor contains synchronization input from GPS; 1pps (pulse per second), to assure precise signal sampling without quantizing errors. Magnetic compensation may be undertaken in real-time on as many as three (3) CS-3 magnetometers, simultaneously. However, if more than three CS-3 magnetometers are used simultaneously then the compensation must be undertaken as a post-mission exercise, in either case using Pico Envirotec's PEI-Comp module; Fig. 2 [5].

PEI-Comp quickly creates a magnetic coefficient file to compensate magnetic data. The source data is the PEI binary data file recorded during a compensation test flight. If the source data is not a Pico Envirotec binary data file, there is a provision to import data from a text file. The input file must contain at least x, y, and z data from a 3-axis fluxgate magnetometer, raw total field magnetometer data, and x and y position coordinates for heading calculations. Usually four sets of coefficients are created one for each of the four cardinal headings.

A Billingsly TFM-100 (or equivalent) Tri-Axial Fluxgate Magnetometer measures the aircraft's attitude during flight, and provides x, y, and z data for recording by the AGIS data acquisition system. As previously mentioned, these data are used for the calculation of the coefficients necessary for magnetic compensation [6].

2.2.2. Airborne Navigation System:

The airborne system of the NMA aircraft is of the model LiNav one, which is a real-time DGPS airborne navigation system, designed by AG-NAV Inc. for line and waypoint surveys for use in helicopter or fixed wing aircraft (Fig. 3). The system provides a real-time presentation of complex positioning information from various types of GPS receivers to the pilot in a transparent and simple format. It is designed specifically for low level flying. MiNav has become the indispensable tool in airborne geophysical operations.

The LiNav system provides accurate guidance to the pilot to fly the preplanned flight lines in a survey area. This system provides all utilities to do necessary things from flight planning to data handling. The built-in editor is used to set up the boundary of a survey area, flight lines and waypoints. Based on the line heading and a reference point, LiNav automatically generates the flight lines which are parallel and evenly spaced inside the survey area. The basic LiNav system consists of a rack-mount console with computer for data processing, recording and storing. A high resolution monochrome LCD moving map display provides real-time viewing of navigation information in variable formats and modes including zooming and auto-centering features. Two-line pilot Indicators provided critical navigation data for the pilot. A compact keyboard on a tray is provided for editing, carrying out diagnostics checks, pre and post flight preparations, more details of specifications and performances in detail [7].

3. Magnetic Compensation:

Two magnetic field sensors are installed on an aircraft [8]. The quantum magnetometer measures the absolute value of the magnetic field with a high precision; the 3-axis flux gate magnetometer measures the magnetic field vector, but its precision is much lower. The quantum sensor can operate with a limited set of magnetic field directions only. There are three direction sets, where the quantum sensor fails to operate: at the two poles and the equator. When the aircraft flies above the earth poles, the field direction is vertical, and its value is independent of the course (in the aircraft coordinates). Therefore, if the sensor is installed correctly, it will not leave the permissible orientation range, independently of the aircraft course. When the aircraft flies above the equator, only four orthogonal flight headings are permissible without changing the sensor orientation (along the tie-lines or along the traverse lines). The magnetometer axis shall be located at an angle of 45 degrees to the magnetic field direction. When setting the sensor orientation, the magnetic declination shall be taken into account, in addition to the route heading.

Fig. (2) : MMS-4 High-sensitivity magnetometer processor with its CS-3 sensor, and Billingsly TFM Tri-axial fluxgate magnetometer.

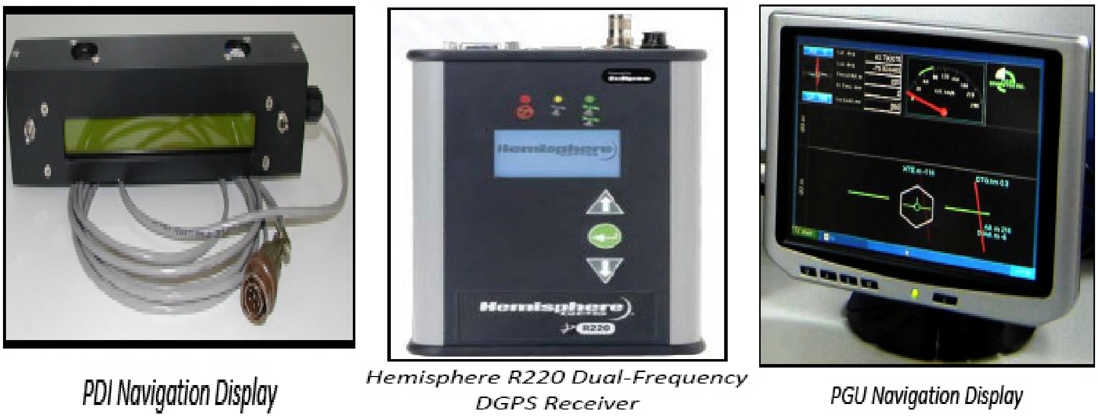

Fig. (3): Airborne Navigation System installed onboard NMA aircraft.

3.0. The Source of the Distortion:

3.1. Hard Component Distortion:

The aircraft causes magnetic field distortion of three types. The first distortion type (called a hard magnetic field component) is simply a constant additional vector component. The main vector may change its direction (in the aircraft coordinates); as the hard component is relatively low, the vector elongation is actually equal to the projection of the hard vector onto the main vector. If the reading of the vector magnetometer is normalized to unity, the considered correction is equal to the scalar product of the intrinsic magnetization vector by the normalized vector of the flux gate magnetometer.

3.2. Soft Component Distortion:

The soft component results from the influence of the magnetic field on the aircraft parts, it depends on the direction of the external magnetic field. Additional magnetic field component appears in the point, where the quantum sensor is mounted; it is described by a 3×3 matrix. In order to determine its contribution to the resultant vector value, the projection of this component onto the main vector shall be found. As the result, a quadratic expression is obtained. Let us present this expression as a 3×3 matrix, whose above-diagonal elements are equal to zero. The elements X*Y and Y*X are equal to each other, they are determined together. As the result, 6 coefficients are obtained. It is again more convenient to use the normalized vector of the fluxgate magnetometer; in this case, the correction will be proportional to the field that is to the value measured by the quantum sensor. Thus, the coefficients obtain clearness and physical sense. When using the considered expression, it shall be multiplied by the field value in the given point and divided by the mean value at the moment of compensation (the difference between the real value and the measured value is neglected).

Let us assume that the quantum sensor is enclosed into a uniform spherical shield, which reduces the magnetic field value equally in all directions. It is evident, that no experiments can help to determine the shielding factor. In other words, after including the compensation, the field values measured using different aircraft are reducible to each other only to within a certain coefficient, close to 1. In addition, the aircraft differ from each other, because the frequencies of their reference crystal oscillators used in the counters are different. Therefore, we must establish a certain additional condition. It is assumed that the field is directed along the axis X is true, so the corresponding correction is equal to zero. As the result, 5 coefficients remain.

4.0. Problem Description:

The maneuver noise can be considered to be caused due to [9]:

1) permanent magnetic field of the aircraft,

2) induced magnetic field of the aircraft in the earth's magnetic field, and

3) magnetic field from eddy currents due to changing orientation of the large metal surfaces in the earth's field.

5.0. Correction Procedures:

Starting from early seventieth, many trials were carried out in order to enhance the gathered airborne magnetic data. In this concern, in 1961, Leliak published a paper outlining a mathematical technique for estimating and removing the effects of an aircraft from magnetic data collected from a several total field sensors [10]. The basis of this technique is a system of linear equations which attempts to represent the permanent, induced and EM effects due to an aircraft as a function of the attitude. Four flight paths are normally flown at high altitude in box wide sides parallel to the proposed survey azimuth with a series of pitch, roll, and yaw movements. The data from these flight paths are then used to determine the 18 coefficients relating to the motions and the linear equation system is then used to move the aircraft's magnetic effects from survey data flown at lower altitude. The altitude of the plane is usually determined from vector fluxgate data from sensors also mounted on the aircraft but attempts are being made to determine attitude from multiple GPS sensors.

It has been shown that the correction model can be represented by a set of linear equations with different distinct terms [11].The problem of determining the coefficients is generally considered as a linear least-squares regression. However, it can also be considered as a cross correlation problem, whereby it is assumed that there is no correlation with the aircraft orientation, and that the orientation of the aircraft can be considered by a set of "monitors" [12, 13]. The "monitors" in the latter method are thus the coefficients associated with the directions cosines and their time derivatives, which can be derived from the three axes fluxgate magnetometer.

In order to calculate the correction coefficient, to be used in the purification of the regular magnetic data, a calibration flight sortie was carried out over a specified area, at relatively high altitude (about 10,000 feet). The chosen area should be relatively magnetically calm. Flight lines are chosen on the four flying line directions. The correction coefficients are ranging from 3 to 30 for each direction separately. Each direction will be explained separately for 3 border transactions.

5.1. Determination of Regional Magnetic Component:

5.1.1. First Direction:

Figure (4) shows the collected magnetic data, for one direction, super- imposed over the aircraft noise, which arise due to movements along the three directions Z, Y, and X ; namely : Pich, roll, and yaw respectively. It clearly shows to the extent of the effect of the aircraft maneuvers.

To remove the regional component, the collected airborne magnetic data are fitted applying the following equation:

$$mag_{fit[p]} = \sum_{n=1}^{n=3} c[n] * p\^{}n \qquad (1)$$

Where:

n : number of the coefficients sufficient for best solution,

c: the coefficient, and

p : value of the detected data.

Applying the different correction coefficients on the collected raw airborne magnetic measurements will produce the data shown in Fig. (5).

Figure (6) shows the difference between the raw airborne magnetic data (Fig. 4) and the fitted data (Fig. 5). The obtained data represent the aircraft maneuver effects, which should be removed during survey from the actual survey magnetic data.

5.2.0. Coefficients for theDetermination of Aircraft Maneuvers:

In the present step, the aircraft maneuvers effect should be determined from the data collected in x, y, and z deviations. In this concern, the data stored on the x_dev, y_dev, and z_dev (Fig. 7), are used during the fitting of the data shown in Fig. (6). applying the following equation:

$$\mathbf{comp_{magnetic[p]}} = (\mathbf{x[p]} * \mathbf{c[1]}) + (\mathbf{y[p]} * \mathbf{c[2]}) + (\mathbf{z[p]} * \mathbf{c[3]}) + \mathbf{c[4]} \ldots\ldots \quad (2)$$

Where :

x[p], y[p], and z[p] are , x, y, and z deviations, and

c[1], c[2], c[3], and c[4] are the extracted coefficients.

Figure (8) shows the fitting motion, from which, Fig. (9) shows those comparative plots between the collected raw magnetic maneuver data and that calculated.

The main target of the present work is to minimize the difference between the measure and calculated data (figure of merit), a look to Fig. (9) insures that, primarily, a figure of merit value of 0.6414 was obtained.

Figure (10) shows the obtained graphs for the other three compensation flying directions after applying the procedures carried out for the first one. Figures 9 and 10, clearly show that, there is still noticeable shift in the corrected data. So they need more fine adjustment.

Figure (11) shows the final results of the investigated correction procedures, where a comparison between raw data (blue), case of only 3 coefficient (magenta), and 30 coefficients (yellow).

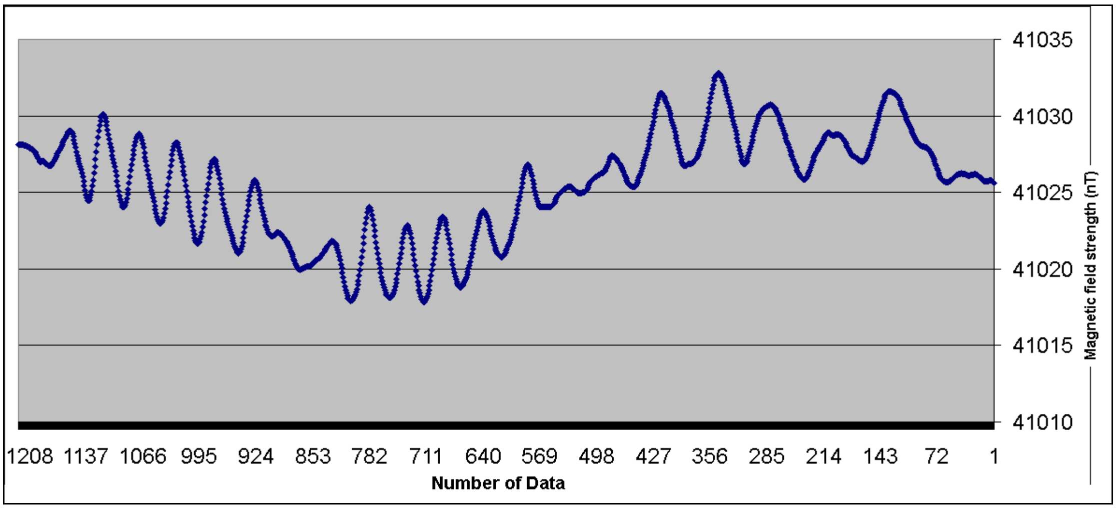

Fig. (4): Airborne magnetic data superimposed over the aircraft noise due to its movements along the three directions (x, y, and z).

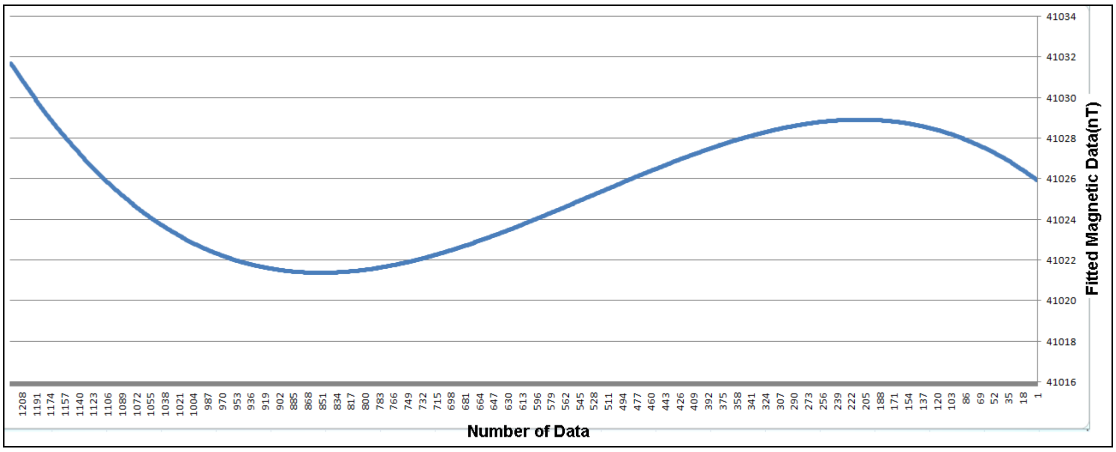

Fig. (5): Fitted magnetic data.

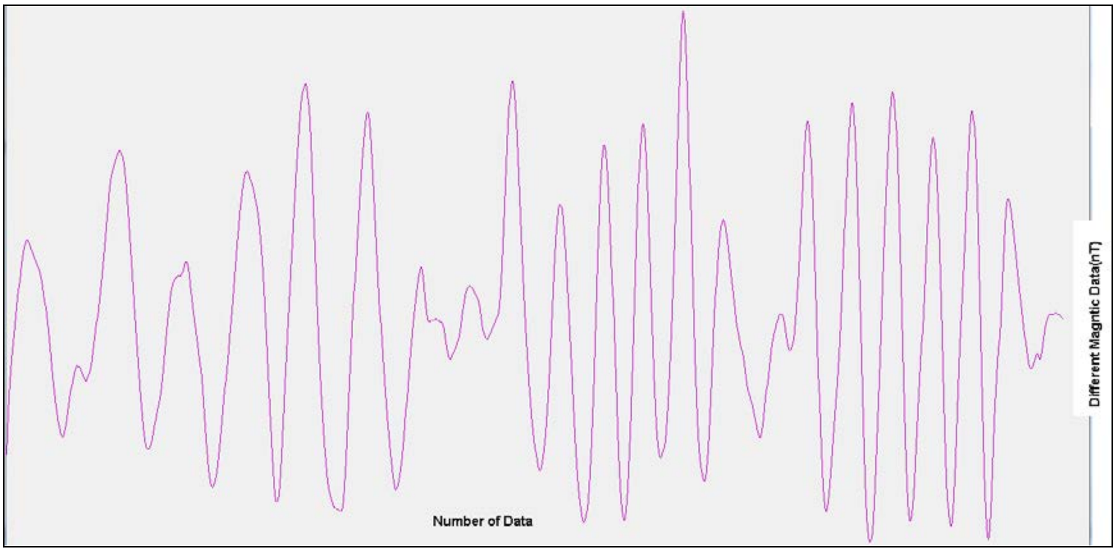

Fig. (6): x, y, and z motions.

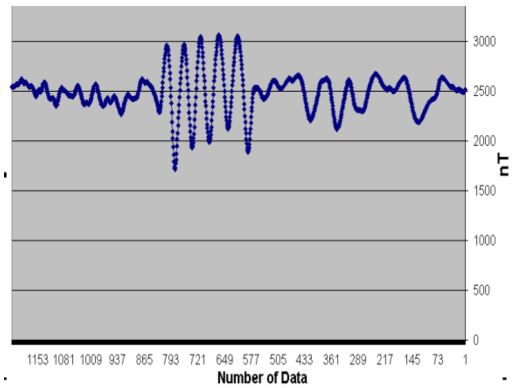

(a)

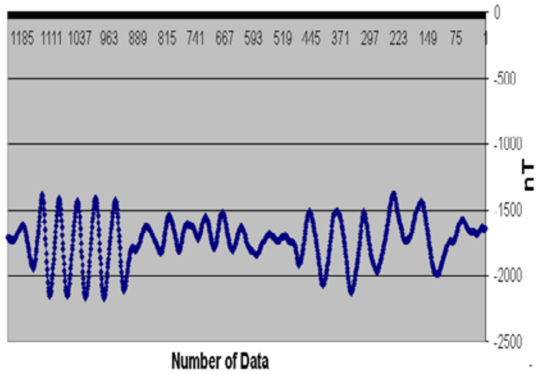

(b)

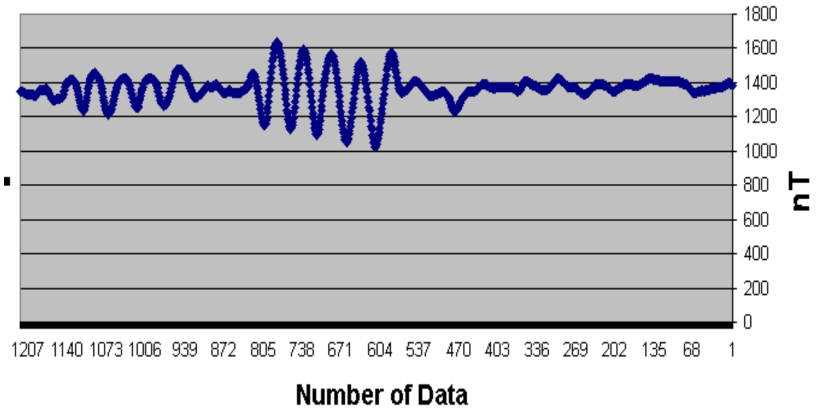

(c)

Fig. (7): x (a), y (b), and z (c) maneuvers direction of the aircraft during compensation flight.

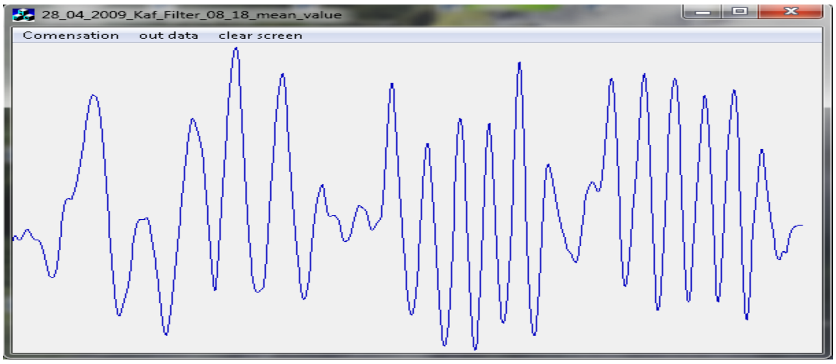

Fig. (8) : Fitted motion.

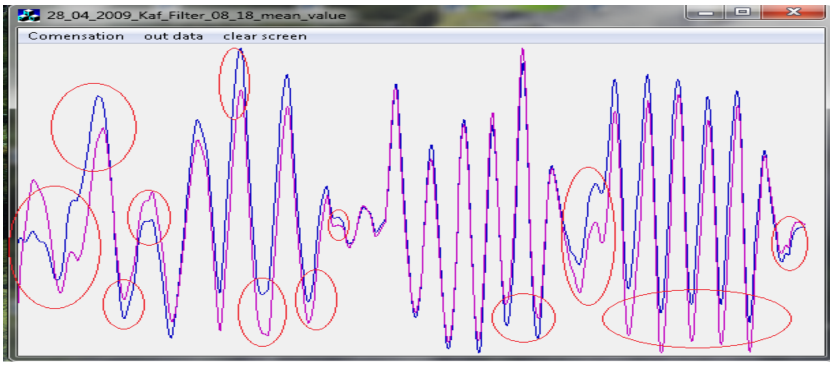

Fig. (9) : The calculated airborne magnetic data (blue) and the measured (magenta).

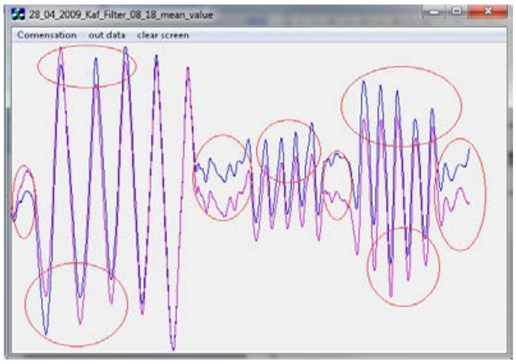

(a)

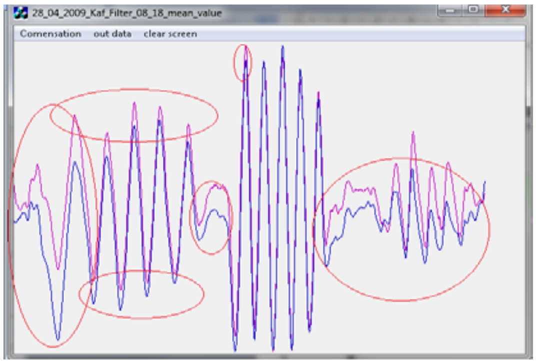

(b)

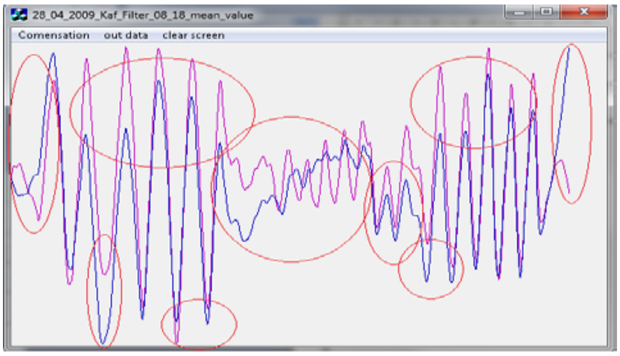

(c)

Fig. (10) : Plots of magnetic data of compensation flights on three directions.

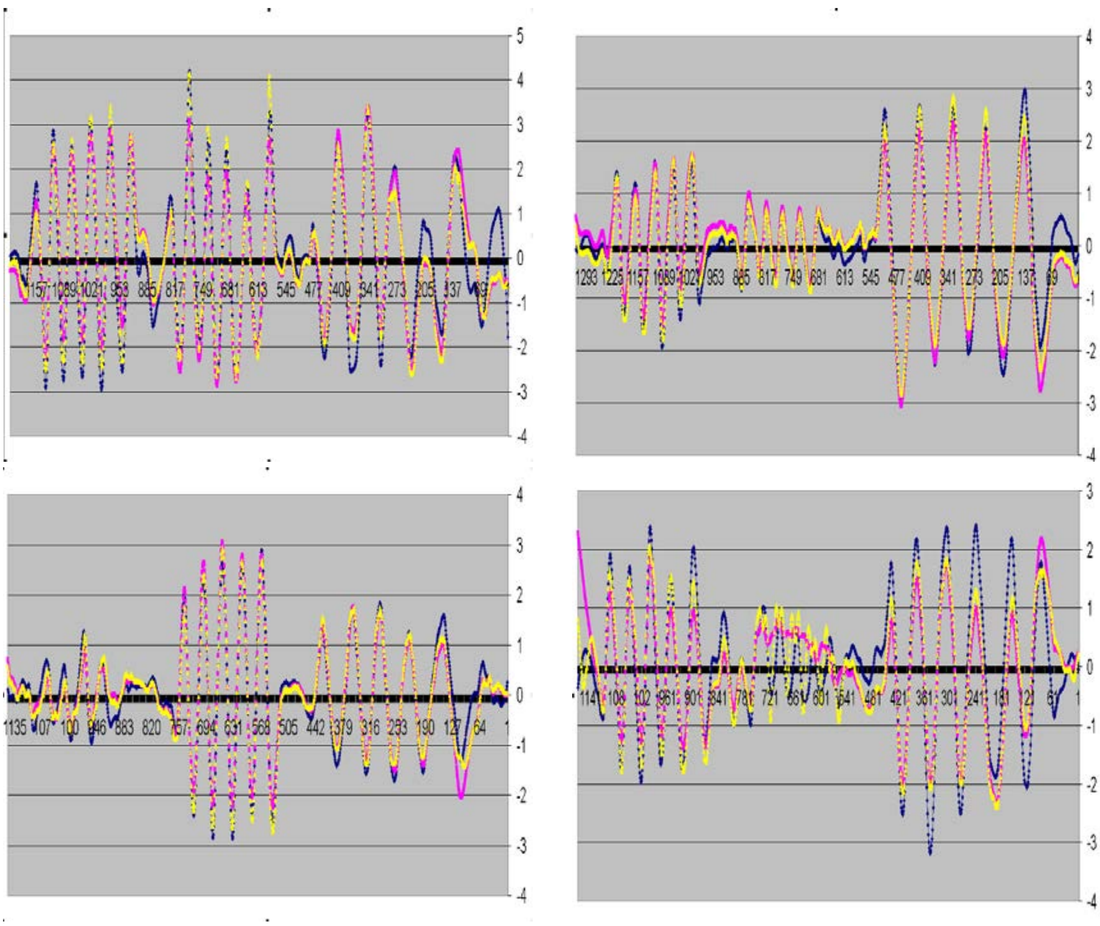

Fig. (11) : Magnetic data of the four direction compensation flights, plotted for raw data (blue), fitted using three coefficients (magenta), and fitted using thirty coefficients (yellow).

Table (1): Figure of merit values calculated at different coefficients number of Equations 3 and 4.

Number of Coefficients of Equation (4): 30	27	24	21	18	15	12	9	6	3	Number of Coefficients of Equation (3)
0.4684	0.5226	0.501	0.508	0.571	0.6063	0.6204	0.618	0.6168	0.6414	4
0.3543	0.3622	0.3687	0.3571	0.3601	0.3754	0.3994	0.4108	0.4698	0.6933	7
[redacted]	0.3525	0.3691	0.3599	0.3870	0.4156	0.4479	0.4535	0.4923	0.7127	10
0.4138	0.4154	0.4393	0.4345	0.4708	0.4927	0.5217	0.5050	0.5457	0.7295	13
0.4157	0.4168	0.4348	0.4194	0.4718	0.4969	0.526	0.5299	0.5821	1.0000	16
0.4247	0.4344	0.4498	0.4395	0.4894	0.5161	0.5407	0.5706	0.6138	0.7207	19
0.6181	0.6294	0.6545	0.6309	0.7308	0.7893	0.7915	0.8621	0.9110	0.7233	22
0.4216	0.4278	0.4445	0.4345	0.4695	0.4975	0.5305	0.5362	0.5767	0.7701	25
0.4726	0.4795	0.4904	0.4847	0.5281	0.5310	0.5486	0.5758	0.5978	0.8158	28
0.4741	0.4778	0.4903	0.487	0.5317	0.5646	0.5919	0.6194	0.6511	0.7172	31
0.524	0.5377	0.5535	0.5501	0.5831	0.6193	0.6375	0.6640	0.7047	0.7332	34
0.4215	0.4304	0.4427	0.4423	0.5006	0.5271	0.5555	0.5640	0.6032	0.6414	37
0.4314	0.44	0.4531	0.4412	0.4974	0.5238	0.5479	0.5762	0.6146	0.6933	40

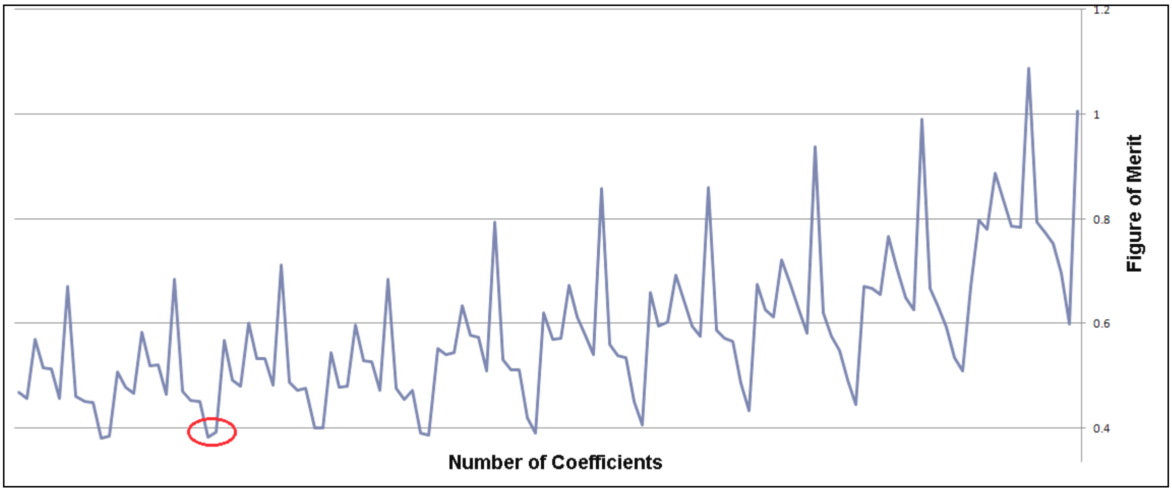

Fig. (12): Figure of merit dependence on the coefficients matrix of equations 3 and 4.

Many trials were carried out in order to test the effect of increasing the number of coefficients on Equation (1). This was carried out in steps of 4, 7, 10, 13, till 40.

$$mag_{fit[p]} = \sum_{n=1}^{n=40} c[n] * p\hat{\ }n \qquad \ldots . (3)$$

On the other hand, considering Equation (2), the number of coefficients increased from 3 up to 30. From which:

$$\begin{aligned} comp_{magnetic[p]} \\ = \\ &= (c[1]*x[p]^7) + (c[2]*y[p]^7) + (c[3]*z[p]^7) \\ &+ (c[4]*x[p]^3*y[p]^3) + (c[5]*x[p]^3*z[p]^3) + (c[6]*z[p]^3*y[p]^3) \\ &+ (c[7]*x[p]^6) + (c[8]*y[p]^6) + (c[9]*z[p]^6) + (c[10]*x[p]^5) \\ &+ (c[11]*y[p]^5) + (c[12]*z[p]^5) + (c[13]*x[p]^4) + (c[14]*y[p]^4) \\ &+ (c[15]*z[p]^4) + (c[16]*x[p]^3) + (c[17]*y[p]^3) + (c[18]*z[p]^3) \\ &+ (c[19]*x[p]^2) + (c[20]*y[p]^2) + (c[21]*z[p]^2) + (c[22]*x[p]) \\ &+ (c[23]*y[p]) + (c[24]*z[p]) + (c[25]*x[p]^2*y[p]^2) \\ &+ (c[26]*x[p]^2*z[p]^2) + (c[27]*z[p]^2*y[p]^2) \\ &+ (c[28]*x[p]*y[p]) + (c[29]*x[p]*z[p]) \\ &+ (c[30]*z[p]*y[p]) \ldots\ldots\ldots\ldots\ldots\ldots (4) \end{aligned}$$

From which, it is clearly shown that the proposed technique was able to an excellent degree to be commonly used on line. Also, Table (1) illustrates the figure of merit values calculated at different number of coefficients used in equations (3 and 4).

Finally, Fig. (12) shows the figure of merit, plotted as a function of number of coefficients, where an optimum figure of merit value of 0.3513, was found to be located at positions (30, 10). Note that, the location values are referred to Equation (4), and Equation (3), respectively.

CONCLUSIONS

The present paper includes a new advanced technique for removal of noises related to aircraft's maneuvers in airborne magnetic surveys. The proposed technique was proved to be simple, needs no long execution time, as well. It proved to enhance the airborne magnetic data, a matter which in turn, could be considered as an addition for its applications on landmines and earth wealth exploration fields.

REFERENCES

[1]. **Smith, B. D., et al.,** " Airborne electromagnetic and magnetic surveys for ground water resources", In Proc. of Exploration 07: 5th Decennial Intr. Conf. on Mineral Exploration" Edited by B. Milkereitc, Denver, USA, pp. 895-899, 2007.

[2]. **M. El-kattan, H. El-Henawy, Ala-Din Kamal, F.A.S. Soliman, A. Salem, and A. Osman,** " Integrated detection of landmines using neutron back-scattering and magnetic gradient techniques ", 22nd Intr. Geophysical Conf. and Exhibition, Brisbane, Australia, 26 - 29 Feb., 2012.

[3]. **M. El - Kattan, A. Salem, F.A.S. Soliman, Ala-din Kamel, Hadia El-Hennawy,** "Micro-controller based neural network for landmine detection using magnetic gradient Data", 4th Intr. Conf. on Intelligent and Advanced Systems, ICIAS2012, pp. 46-50, Kuala Lumpur, Malaysia, 12-14 June 2012.

[4] **Salem, A., Ushijima, K., Gamey, T., J., and Ravat, D.,** " Automatic detection of UXO from airborne magnetic data using a neural network,"Subsurface Sensing Technologies and Applications, Vol. 2, No. 3, July 2001.

[5] PicoEnvirotec, Inc., www.picoenvirotec.com/

[6] Billingsly, AeroSpace and Defense, mcphar international.com/.../ismap-discussion_ 2b8489fe9a0006daa6003...

[7] AG-Nav, GPS Precision Navigation, www.agnav.com/

[8] Compensation of Airborne Data, drobotenko.com/ demagnitor.htm

[9] **Luyendyk, A.P.,** " Processing of airborne magnetic data", Medley, AGSO Journal of Australian Geology Geophysics ,Vol. 17, No. 2, Publisher: Australian Gov. Publ. Service, pp. 31-38, 1997.

[10] **Leliak, P.,** "Identification and evaluation of magnetic field sources of magnetic airborne detector MAD equipped aircraft", IRA Transactions on Airspace and Navigational Electronics, Vol. 8, pp.95-105, Sept. 1961.

[11] **Leach, Barrie W.,** "Aeromagnetic compensation as a linear regression problem ", NAE NAE report, 1980.

[12] **Lacoste, Lucien, J.,** " correlation method for evaluating and correcting shipboard gravity data", geophysics, Vol. 38, No. 4, pp. 701-709, 1973.

[13] **C. Cafforio**, " Motion compensation processing of airborne data ", igarss2008.com/ Abstracts/pdfs/ 2250.pdf.